



**HAL**  
open science

## Calculation of conducted EMI generated by single-ended primary inductance converter

Kahina Mostefaoui-Kasri, Yacine Azzouz, Mohamed Benbouzid, Anne Louis, Bélahcène Mazari, Philippe Eudeline

### ► To cite this version:

Kahina Mostefaoui-Kasri, Yacine Azzouz, Mohamed Benbouzid, Anne Louis, Bélahcène Mazari, et al.. Calculation of conducted EMI generated by single-ended primary inductance converter. International Review of Electrical Engineering, 2012, 7 (3), pp.4469-4479. hal-00926436

**HAL Id: hal-00926436**

**<https://hal.science/hal-00926436>**

Submitted on 9 Jan 2014

**HAL** is a multi-disciplinary open access archive for the deposit and dissemination of scientific research documents, whether they are published or not. The documents may come from teaching and research institutions in France or abroad, or from public or private research centers.

L'archive ouverte pluridisciplinaire **HAL**, est destinée au dépôt et à la diffusion de documents scientifiques de niveau recherche, publiés ou non, émanant des établissements d'enseignement et de recherche français ou étrangers, des laboratoires publics ou privés.

# Calculation of Conducted EMI Generated by Single-Ended Primary Inductance Converter

K. Mostefaoui-Kasri<sup>1</sup>, Y. Azzouz<sup>1</sup>, M.E.H. Benbouzid<sup>2</sup>, A. Louis<sup>3</sup>, B.Mazari<sup>3</sup> and P. Eudeline<sup>4</sup>

**Abstract** – This paper deals with the problem of conducted electromagnetic disturbances generated by a single-ended primary inductance converter (SEPIC) switching power supply for radar applications. In the proposed model the passive components are replaced by their high frequency (HF) equivalent models and the active elements by the interference sources. The six windings transformer, which is one of the passive elements of the switching power supply allows the adaptation of voltage levels and provides galvanic isolation between input and output. It will be modeled by: a simplified model and then by a model taking into account coupling between the leakage inductances. The accuracy of each model is established by comparing the simulation results of conducted electromagnetic interference (EMI) to measurement results. Copyright © 2012 Praise Worthy Prize S.r.l. - All rights reserved

**Keywords:** electromagnetic interference (EMI), emission, frequency domain analysis, measurement, power electronics.

## I. Introduction

The increase of switching frequency in power converters allows reducing the volume of power supplies. However, this increase in frequency generates disturbances, mostly due to high  $di/dt$  loops and high  $dv/dt$  nodes in power stages, on the mains network. To meet the standards that define the limits of conducted disturbances supported by the network, it is highly recommended to quantify these disturbances allowing to have a pre-qualification of conducted emissions before design.

Numerical computation is an effective way of study the high frequency (HF) behavior of power converters structures in time and a frequency domains. It allows the designer to reduce the number of prototypes during the design phases. Moreover, the use of these tools allows a better understanding of electromagnetic phenomena in power converters and better system optimisation.

Time domain simulations offer good results for simple systems. However, for complex systems, simulations become very slow and discrepancies start occurring. Given the complexity of the studied power supply (multi-winding transformer, the presence of multiple filters, large number of components) and in order to avoid the drawbacks of time-domain methods, a frequency-domain simulation has been chosen.

The modelling presented in this paper consists of: modeling of the active elements by interference sources (voltage), replacing passive components such as capacitors, coils and resistors by their HF equivalent models, establishing the equivalent diagram of the overall structure and calculating the conducted electromagnetic disturbances that can interfere with the mains network.

After presenting the studied power supply, this paper focuses on the calculation of disturbances in differential-

mode and common-mode for two HF transformer models: the first one without leakage inductances coupling and the other with this coupling. The results are then compared with measurements for validation.

## II. Studied switching power supply

The Fig 1 shows the classical diagram of a single-ended primary inductance converter (SEPIC). This converter lowers the voltage from 320 V (rectified mains voltage) to 56 V. Its switching frequency is 100 kHz and the transmitted power is 1350 W.

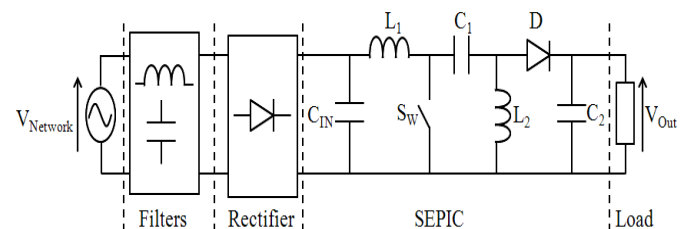


Fig 1 SEPIC topology, including filters and rectifier

In the studied structure:

- $L_2$  is replaced by a transformer to decrease the output voltage and ensure galvanic isolation.
- In order not to exceed the maximum current allowable by the diode D, a current division was adopted by using a multi-windings transformer multiplying the number of secondary windings by 4.
- The coil  $L_1$  is placed on the same core as the transformer because it was found that their voltages have the same instantaneous values, and it allows a significant volume reduction.

- The switch SW is composed of three MOSFETs (MTW10N100E) put in parallel for two reasons: firstly, dividing the current through each MOSFET, and secondly, reducing the equivalent impedance value of the whole switch.

Such modification of the basic structure make it much more complex (fig 2) and prevent us from an easy EMC study.

Indeed, in addition to the items cited above, the converter features storage and filtering capacities :  $C_{IN}$ ,  $C_1$  et  $C_2$ , bridge rectifier, RC circuits protection at the diodes terminals and filters at the power supply entry.

### III. Active component modeling

To analyze this power supply in frequency domain, both in differential and common modes, we replace non-linear and time dependent MOSFETs and diodes by [1]:

- a voltage source which is the voltage measured at its terminals VMOSFET (VDiode) (fig 3, fig 4)
- its parasitic inductances  $L_D$ ,  $L_S$  ( $L_A$ ,  $L_K$ ) given by the manufacturers;
- and a dynamic impedance identified by measurement with behave as : an inductance during conduction ( $L_{D_{dyn}}$ ), zero impedance while switching and capacitance while blocking ( $C_{D_{dyn}}$ ) as identified by the impedance measurement.

Over a switching period T, we find that the measured voltage can be decomposed into several mathematical functions (TABLE I). The model then consists of replacing the voltage source representing the MOSFETS (Diodes) by mathematical equations that reproduce the same waveforms. These equations will be transposed later in the frequency domain (using Laplace transforms) as described in TABLE II.

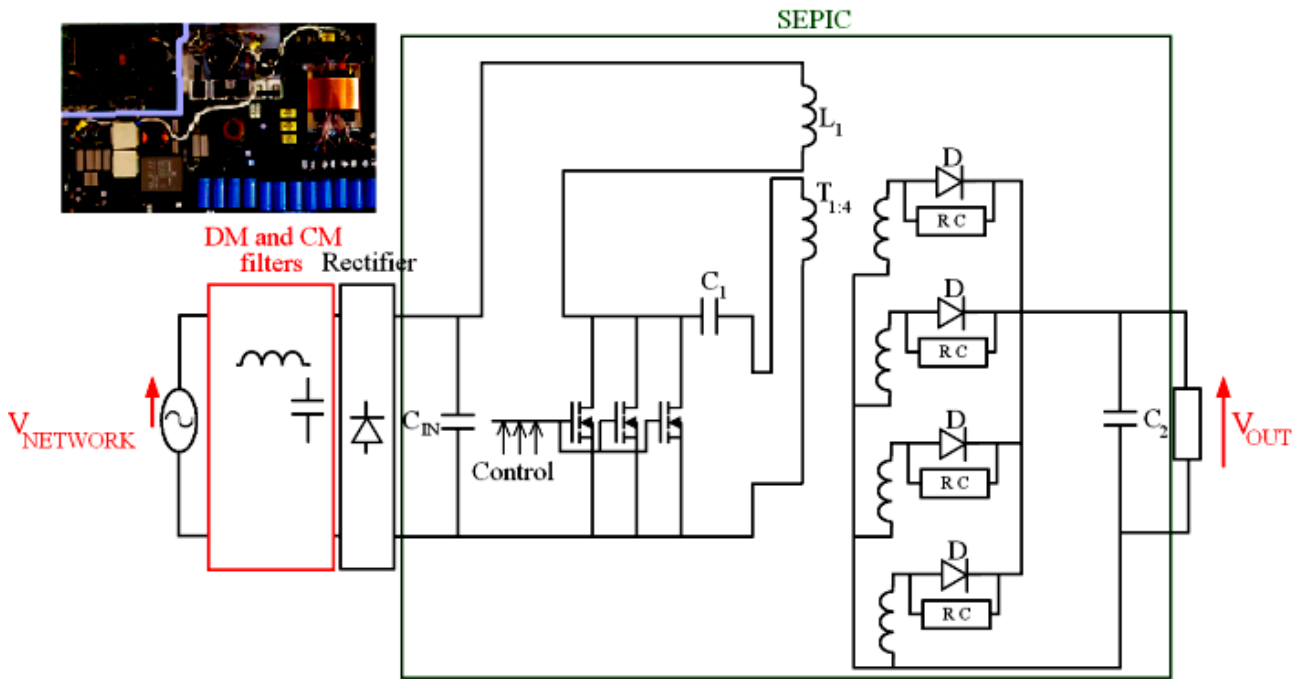


Fig 2 Studied SEPIC

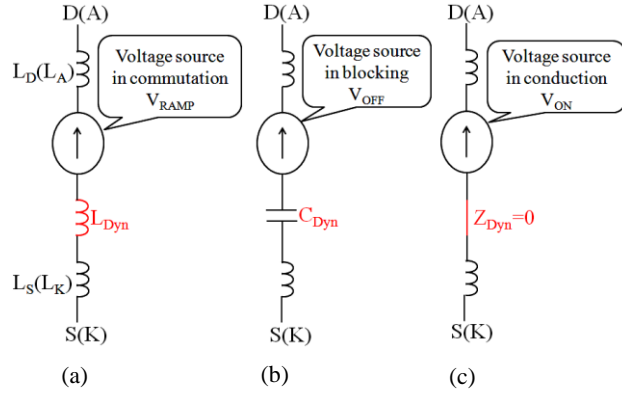


Fig 3 Equivalent model for MOSFET (diode) while: (a) switching, (b) blocking and (c) conducting

TABLE I  
FORMULATION OF VOLTAGE WAVEFORM AT THE TRANSISTOR  
TERMINALS IN RELATION WITH ITS STATE

Voltage wave at the transistor terminals	Analytic equations
<p>In the time interval <math>[T_0 - T_r]</math></p>	$V_{rampes-OFF} = A_1 U(t - T_0)$ $+ \frac{A_2 - A_1}{T_r - T_0} \cdot (t - T_0) U(t - T_0)$ $- \frac{A_2 - A_1}{T_r - T_0} \cdot (t - T_r) U(t - T_r)$ $- A_2 U(t - T_r)$
<p><math>[T_r - T_1]</math></p>	$V_{OFF1} = A_2 U(t - T_r)$ $- K_1 \cdot e^{-\alpha(t - T_r)} \cdot \sin(\beta(t - T_r))$ $+ K_2 \cdot e^{-\alpha(t - T_1)} \cdot \sin(\beta(t - T_1))$ $- A_2 U(t - T_1)$
<p><math>[T_1 - T_{f1}]</math></p>	$V_{OFF2} = A_2 U(t - T_1)$ $- \frac{A_2 - A_3}{T_{f1} - T_1} \cdot (t - T_1) U(t - T_1)$ $+ \frac{A_2 - A_3}{T_{f1} - T_1} \cdot (t - T_{f1}) U(t - T_{f1})$ $- A_3 U(t - T_{f1})$

<p><math>[T_{f1} - T_2]</math></p>	$V_{OFF3} = A_3 U(t - T_{f1})$ $- K_3 \cdot \sin(2\pi f(t - T_{f1}))$ $+ K_3 \cdot \sin(2\pi f(t - T_2))$ $- A_3 U(t - T_2)$
<p><math>[T_2 - T_{f2}]</math></p>	$V_{rampes-ON} = A_3 U(t - T_2)$ $- \frac{A_3}{T_{f2} - T_2} \cdot U(t - T_2)$ $+ \frac{A_3}{T_{f2} - T_2} \cdot U(t - T_{f2})$ $- A_3 U(t - T_{f2})$
<p><math>[T_{f2} - T]</math></p>	$V_{ON} = A_4 U(t - T_{f2})$ $- A_2 U(t - T)$

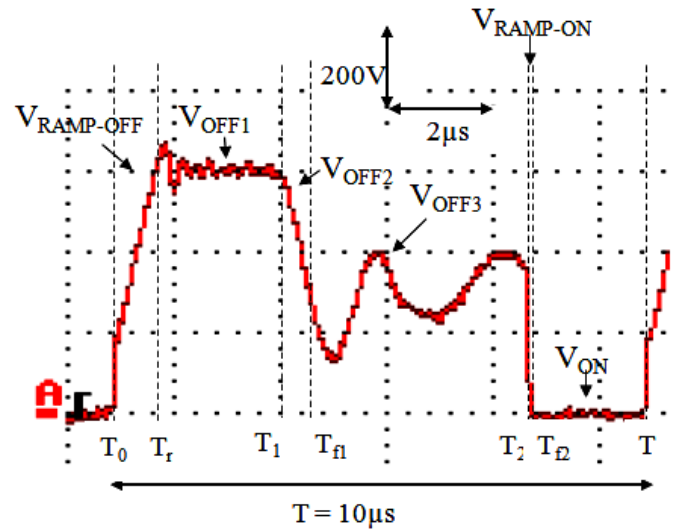


Fig 4 Measured voltage waveform of the transistor.

TABLE II  
FORMULATION OF VOLTAGE WAVEFORMS IN FREQUENCY  
DOMAIN

$V_{rampes-OFF}$	$\frac{1}{p} (A_1 \cdot e^{-T_0 \cdot p} - A_2 \cdot e^{-T_r \cdot p}) +$ $\frac{A_2 - A_1}{T_r - T_0} \cdot \frac{1}{p^2} (e^{-T_0 p} - e^{-T_r p})$
$V_{OFF1}$	$A_2 \cdot \frac{1}{p} (e^{-T_r p} - e^{-T_1 p}) -$ $\frac{\beta}{(p+a)^2 + \beta^2} \cdot (K_1 e^{-T_r p} - K_2 e^{-T_1 p})$

$V_{OFF2}$	$\frac{1}{p} (A_2 \cdot e^{-T1 \cdot p} - A_3 \cdot e^{-Tf1 \cdot p}) -$ $\frac{A_2 - A_3}{p} \cdot \frac{1}{Tf1 - T1} (e^{-T1 \cdot p} - e^{-Tf1 \cdot p})$
$V_{OFF3}$	$A_3 \cdot \frac{1}{p} (e^{-Tf1 \cdot p} - e^{-T2 \cdot p}) -$ $K_3 \cdot \frac{2\pi f}{(2\pi f)^2 + p^2} (e^{-Tf1 \cdot p} - e^{-T2 \cdot p})$
$V_{rampes-ON}$	$A_3 (e^{-T2 \cdot p} - e^{-Tf2 \cdot p}) -$ $\frac{A_3}{Tf2 - T2} (e^{-T2 \cdot p} - e^{-Tf2 \cdot p})$

#### IV. Capacitor and resistor model

In High Frequency, the passive components have frequency-dependent behavior [2]-[3]-[4]. The HF model is obtained by impedance measurements in the frequency range of 100 kHz to 30 MHz.

At the end of each measurement, an equivalent electrical model combining inductance, resistances and capacities is established (fig 5). This model needs parameters identification, using numerical methods.

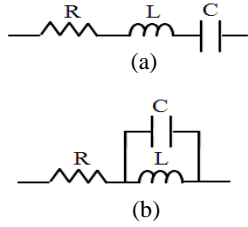


Fig 5 HF equivalent circuit model of capacitor (a) and resistor (b)

To validate the calculation, for example, a comparative study between the measured impedance of the filter capacitor (using a HP 4294 impedance analyzer) and a computed value (from the equivalent circuit diagram) was performed. We note a good agreement between measurement and calculation, which validates the model of this capacitor.

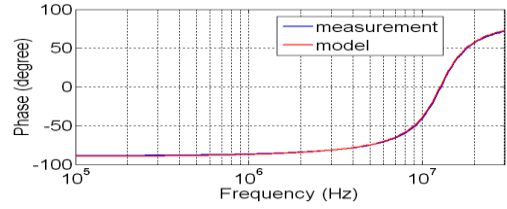
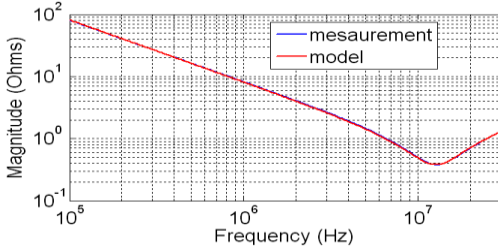


Fig 6 Filter capacitor impedance, Measurement and equivalent model.

#### V. Transformer model without leakage inductors couplers

The studied transformer converts a voltage from 320 V to 56 V and provides galvanic isolation between its input and outputs.

It consists of (Fig 7):

- a transformer T1-4, containing a primary winding 3-4 and four secondary windings;
- and a storage coil  $L_{1-2}$ , placed on the same transformer core.

These two elements listed above have been modeled separately. The coupling between the coil  $L_{1-2}$  and the transformer primary winding has been modeled through their mutual impedance.

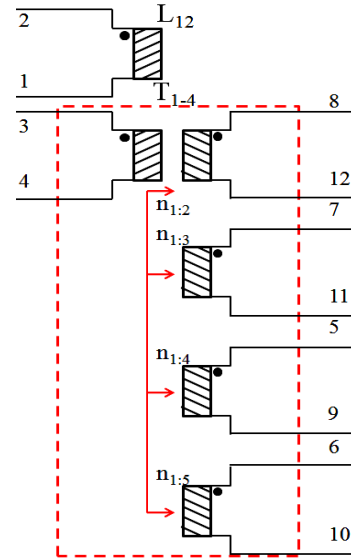


Fig 7 SEPIC Transformer

##### V.1 Inductor $L_{1-2}$ model

The inductor 1-2 is modeled by:

- the impedance  $Z_{L1-2}$  measured cross its terminals,
- and its mutual impedance  $Z_{M1-2}$  measured cross the terminals of both 1-2 and 3-4 parallel coils terminals.

Fig 8 shows equivalent electrical circuits of impedance  $Z_{L1-2}$  and mutual impedance  $Z_{M1-2}$ . The choice of these circuits is confirmed by comparisons between calculated impedances and measurements (Fig 9, Fig 10).

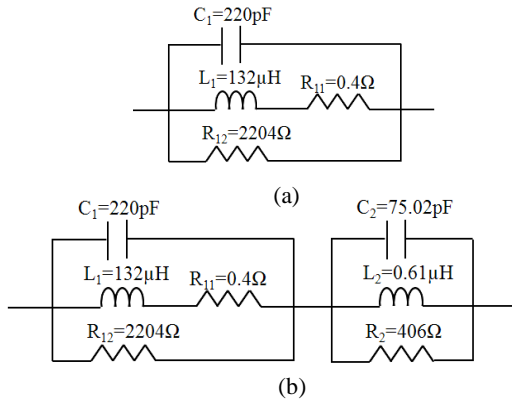


Fig 8 Equivalent electrical circuits: a) impedance, b) mutual impedance

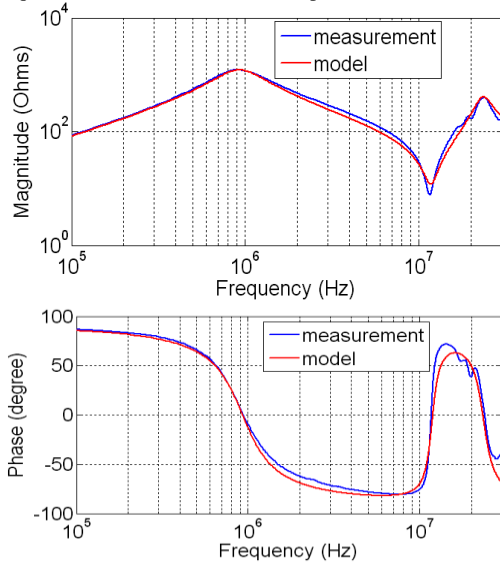


Fig 9 Impedance  $Z_{L1-2}$ , measurement and model

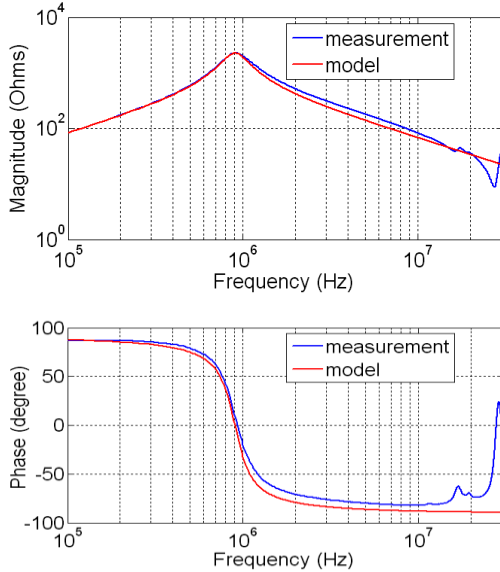


Fig 10 Mutual impedance  $Z_{M1-2}$ , measurement and model

## V.2 Transformer T1-4 model without parasitic capacitances

The HF equivalent circuit of the transformer consists ofn [5]:

- a magnetic part representing the currents circulation
- and a capacitive part allowing the circulation of parasitic currents to be dealt with later in C)

The resulting circuits are composed of inductive elements and couplers allowing the representation of electric and magnetic links existing between the different windings. The extraction of these elements is based on measurements using the impedance analyzer HP 4294 (40 Hz-110 MHz).

The equivalent circuit of the transformer T1-4 without parasitic capacitances is represented by (Fig 11):

- 5 inductors : magnetising inductor  $L_m$ , and secondary leakage inductances  $L_{f1}$ ,  $L_{f2}$ ,  $L_{f3}$  and  $L_{f4}$
- and 4 principal couplers ( $n_{1:2}$ ,  $n_{1:3}$ ,  $n_{1:4}$  and  $n_{1:5}$ )

The inductances and principal couplers are calculated directly from impedance measurements (TABLE III). Nine parameters need to be identified, which requires nine independent impedance measurements ( $Z_{m1} \dots Z_{m9}$ ), include:

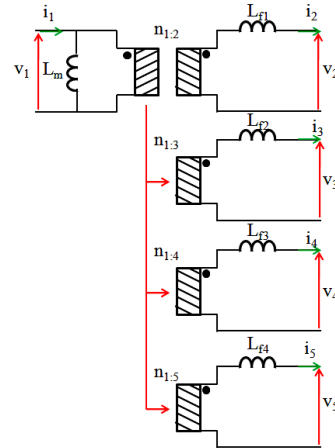


Fig 11 Equivalent circuit of transformer T1-4 without leakage inductors couplers and without parasitic capacitances

- 5 measurements without short-circuit ( $Z_{m1}$ ,  $Z_{m6}$ ,  $Z_{m7}$ ,  $Z_{m8}$  and  $Z_{m9}$ ) ;
- and 4 measurements with one short-circuit ( $Z_{m2}$ ,  $Z_{m3}$ ,  $Z_{m4}$  and  $Z_{m5}$ )

TABLE III  
INDUCTANCES MEASUREMENT CONFIGURATIONS

Measure	Inductors and couplers	view of the winding	With
$Z_{m1}$	$L_m = \frac{Z_{m1}}{2\pi f} \Big _{\varphi=\pi/2}$	3-4	$i_2 = i_3 = i_4 = i_5 = 0$
$Z_{m2}$	$L_{f1} = \frac{Z_{m2}}{2\pi f} \Big _{\varphi=\pi/2}$	8-12	$i_3 = i_4 = i_5 = 0$ and $v_1 = 0$

$Z_{m3}$	$L_{f2} = \frac{Z_{m3}}{2\pi f} \Big _{\varphi=\pi/2}$	7-11	$i_2 = i_4 = 0$ $i_5 = 0$ and $v_1 = 0$
$Z_{m4}$	$L_{f3} = \frac{Z_{m4}}{2\pi f} \Big _{\varphi=\pi/2}$	5-9	$i_2 = i_3 = 0$ $i_5 = 0$ and $v_1 = 0$
$Z_{m5}$	$L_{f4} = \frac{Z_{m5}}{2\pi f} \Big _{\varphi=\pi/2}$	6-10	$i_2 = i_3 = 0$ $i_4 = 0$ and $v_1 = 0$
$Z_{m6}$	$n_{1:2} = \sqrt{\frac{\frac{Z_{m6}}{2\pi f} \Big _{\varphi=\pi/2} - L_{f1}}{L_m}}$	8-12	$i_1 = i_3 = 0$ $i_4 = i_5 = 0$
$Z_{m7}$	$n_{1:3} = \sqrt{\frac{\frac{Z_{m7}}{2\pi f} \Big _{\varphi=\pi/2} - L_{f2}}{L_m}}$	7-11	$i_1 = i_2 = 0$ $i_4 = i_5 = 0$
$Z_{m8}$	$n_{1:4} = \sqrt{\frac{\frac{Z_{m8}}{2\pi f} \Big _{\varphi=\pi/2} - L_{f3}}{L_m}}$	5-9	$i_1 = i_2 = 0$ $i_3 = i_5 = 0$
$Z_{m9}$	$n_{1:5} = \sqrt{\frac{\frac{Z_{m9}}{2\pi f} \Big _{\varphi=\pi/2} - L_{f4}}{L_m}}$	6-10	$i_1 = i_2 = 0$ $i_3 = i_4 = 0$

In Fig 12, the example of  $Z_{m1}$  impedance measurement: the magnetizing inductance is deduced from the inductive part ( $\varphi = \pi/2$ ) of  $Z_{m1}$ . It is calculated at:  $f = 100$  kHz,

$$L_m = \frac{z_{m1}}{2\pi f} = 132 \mu H$$

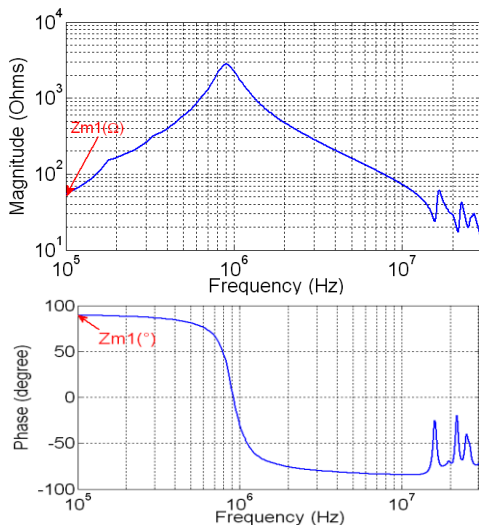


Fig 12 Magnetizing inductance measurement

The other parameters representing magnetic coupling ( $L_{f1}$ ,  $L_{f2}$ ,  $L_{f3}$ ,  $L_{f4}$ ,  $n_{1:2}$ ,  $n_{1:3}$ ,  $n_{1:4}$  and  $n_{1:5}$ ) are calculated from impedance measurements cited in TABLE III.

### V.3 Transformer T1-4 model with parasitic capacitances

To take into account the HF behavior, we now integrate the parasitic capacitances (fig 13)

- windings :  $C_1, C_6, C_7, C_8$  and  $C_9$ ;
- and inter-windings :  $C_2, C_3, C_4, C_5, C_{10}, C_{11}$  and  $C_{12}$

The schematics become more complex and more elements need to be identified.

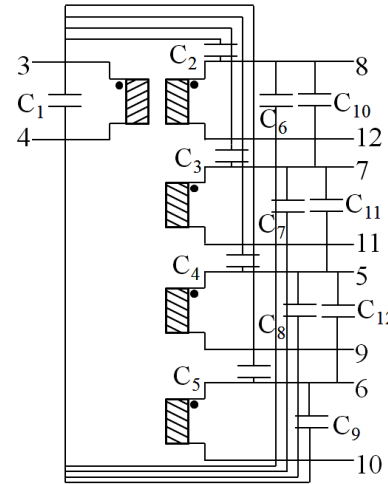


Fig 13 Equivalent circuit of the transformer T1-4 without leakage inductances couplers

These capacitances are identified from the system of equations obtained by impedance measurements (TABLE IV). To avoid a second order system, measurements are done by short-circuiting the largest possible number of capacitances.

TABLE IV  
MEASUREMENT CONFIGURATIONS OF PARASITIC CAPACITANCES AND RESULTING EQUATIONS

Parasitic capacitances	measurement configurations
$C_1 + C_2 + C_3 + C_4 + C_5$ $= \frac{1}{Z_{m1} \cdot 2\pi f} \Big _{\varphi=\pi/2}$	
$C_2 + C_3 + C_4 + C_5 + C_6 + C_7 + C_8 + C_9 = \frac{1}{Z_{m2} \cdot 2\pi f} \Big _{\varphi=\pi/2}$	
$C_2 + C_6 + C_{10} = \frac{1}{Z_{m3} \cdot 2\pi f} \Big _{\varphi=\pi/2}$	

$C_3 + C_7 + C_{10} + C_{11} = \frac{1}{Z_{m4} \cdot 2\pi f} \Big _{\varphi = -\pi/2}$	
$C_3 + C_7 + C_{10} + C_{11} = \frac{1}{Z_{m5} \cdot 2\pi f} \Big _{\varphi = -\pi/2}$	
$C_5 + C_9 + C_{12} = \frac{1}{Z_{m6} \cdot 2\pi f} \Big _{\varphi = -\pi/2}$	
$C_1 + C_3 + C_4 + C_5 + C_{10} = \frac{1}{Z_{m7} \cdot 2\pi f} \Big _{\varphi = -\pi/2}$	
$C_1 + C_4 + C_6 + C_7 + C_{11} = \frac{1}{Z_{m8} \cdot 2\pi f} \Big _{\varphi = -\pi/2}$	
$C_1 + C_5 + C_6 + C_7 + C_8 + C_{12} = \frac{1}{Z_{m9} \cdot 2\pi f} \Big _{\varphi = -\pi/2}$	
$C_1 + C_6 + C_7 + C_8 + C_9 = \frac{1}{Z_{m10} \cdot 2\pi f} \Big _{\varphi = -\pi/2}$	
$C_3 + C_4 + C_5 + C_7 + C_8 + C_9 + C_{10} = \frac{1}{Z_{m11} \cdot 2\pi f} \Big _{\varphi = -\pi/2}$	
$C_4 + C_5 + C_8 + C_9 + C_{11} = \frac{1}{Z_{m12} \cdot 2\pi f} \Big _{\varphi = -\pi/2}$	

The example of the first measurement  $Z_{m1}$  (TABLE IV) is given in Fig 14. The value of parasitic capacitance is deduced at:  $f = 13.65 \text{ MHz}$ ,  $C_{m1} = \frac{1}{Z_{m1} \cdot 2\pi f} = 369 \text{ pF}$

This value is the sum of parasitic capacitances which gives the first equation of the system:

$$C_{m1} = C_1 + C_2 + C_3 + C_4 + C_5 = 369 \text{ pF} \quad (1)$$

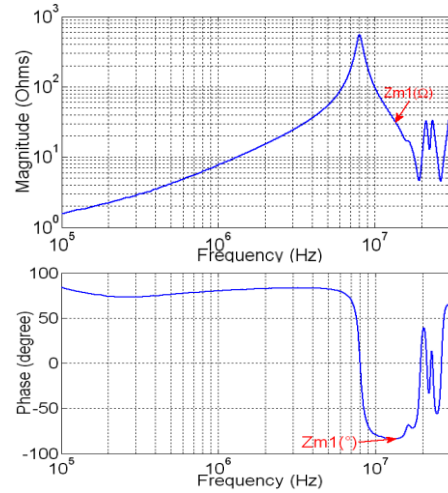


Fig 14 Impedance measurement  $Z_{m1}$

With the 11 other measurements ( $Z_{m2} \dots Z_{m12}$ ), we obtain a system of 11 equations with 11 unknowns. The values of parasitic capacitances are obtained by solving the equations system.

## VI. Measure and calculation of disturbances in differential-mode and common-mode

### VI.1 Spectrum measurements

We distinguish two classes of conducted disturbances:

- those of common-mode (CM), which are spread mainly between live, neutral and earth via parasitic capacitances;
- and the differential-mode (DM), which spreads between live and neutral.

In this study, measurements were made using a clamp-on ammeter F 52 (100 kHz-500 MHz).

The configuration shown in Fig 15 measures the CM current directly in  $\text{dB}\mu\text{V}$ . The DM current, it is calculated by dividing the measured current by two.

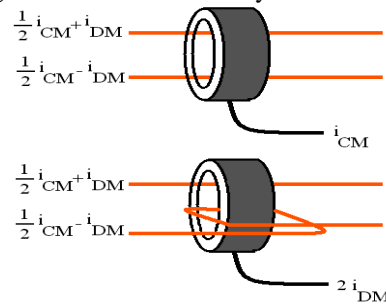


Fig 15 Measurement configurations of common-mode noise and differential-mode noise

According to standards, calculated values in  $\text{dB}\mu\text{A}$  must be recalculated in  $\text{dB}\mu\text{V}$  by 2:

$$I_{\text{dB}\mu\text{V}} = 27.958 + I_{\text{dB}\mu\text{A}} + Z_{\text{pince}} \quad (2)$$

Where:

$I_{dB\mu V}$  = disturbance spectrum;

$I_{dB\mu A}$  = disturbance spectrum observed on the spectrum analyzer;

$Z_{pince}$  = clamp impedance.

In Fig 16 we show the CM and DM measured disturbances spectrums.

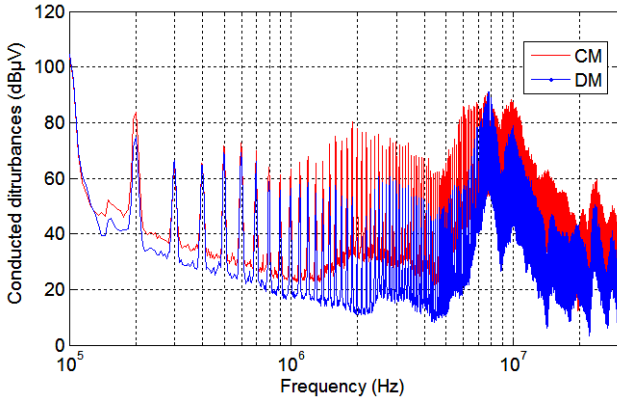


Fig 16 Conducted disturbances spectrums

These measurements will be confronted to calculated disturbance.

## VI.2 Calculation and comparison

For convergence reasons and to save simulation time, we have preferred calculating the disturbances in the frequency domain.

After establishing the complete power supply equivalent circuit, by replacing all components by their models, we obtain a mesh called harmonic model (fig 17), which is then transposed in the form of a square matrix (3) regrouping the equations from Kirchhoff laws.

$$[Z]*[I]=[V] \quad (3)$$

Where :

$[Z]$  = system impedance matrix  $[\Omega]$

$[I]$  = vector of unknown currents  $[A]$

$[V]$  = vector of excitation sources  $[V]$

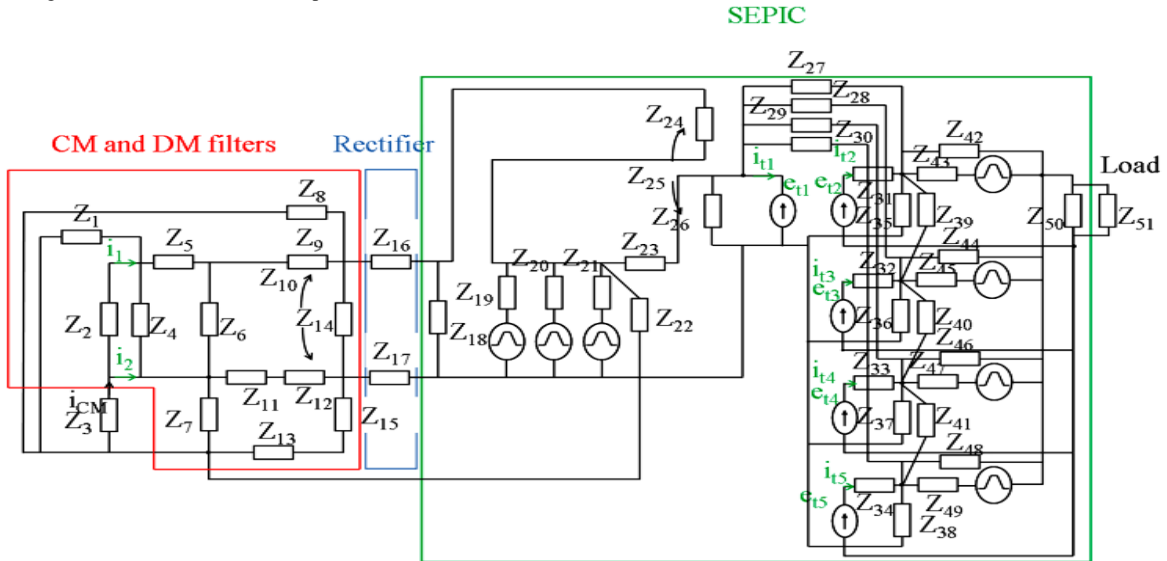


Fig 17 Harmonic model of SEPIC HF equivalent circuit

The following step consists of estimating the DM and CM currents to be estimated solving the matrix system using MATLAB. Indeed, the current vector  $[I]$  especially contains  $i_{MC}$ ,  $i_1$ ,  $i_2$  currents. The DM current is then calculated as a function of  $i_1$  and  $i_2$  by:

$$I_{md} = \frac{(I_1 + I_2)}{2} \quad (4)$$

Multiplying the current by  $50 \Omega$ , we find the value of electromagnetic disturbances in  $dB\mu V$ . Fig 18 and Fig 19 show a comparison between computed spectral envelope and measured spectrum, in differential-mode and common-mode respectively.

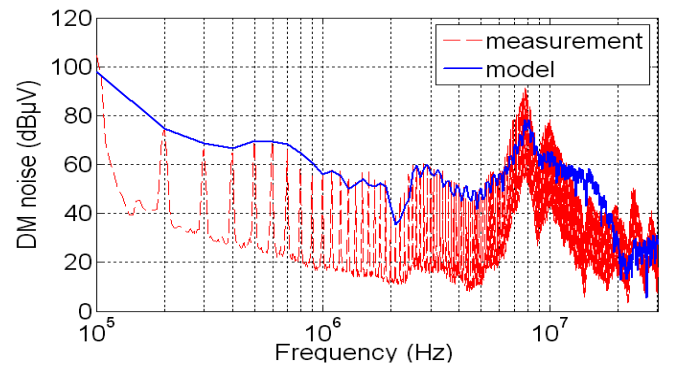


Fig 18 Differential mode noise comparison (model and measurement)

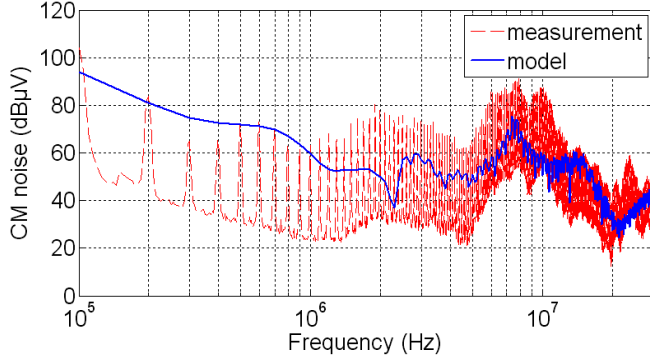


Fig 19 Common mode noise comparison (model and measurement)

For differential-mode calculation, we note a good agreement between calculated spectral envelope and measured spectrum disturbances. However, for common-mode calculation, we note a discrepancy. That is why a second model taking into account the coupling of transformer  $T_{1:4}$  leakage inductances was adopted.

## VII. Transformer model with leakage inductances coupling and validation

In this model, coupling from leakage inductances is taken into account in addition to inductors, main coupling and parasitic capacitance. The equivalent diagram of this model (fig 20) then contains : 5 inductances ( $L_{f1}$ ,  $L_{f2}$ ,  $L_{f3}$  and  $L_{f4}$ ), 4 principal couplers ( $n_{1:2}$ ,  $n_{1:3}$ ,  $n_{1:4}$  and  $n_{1:5}$ ), 3 couplers for the rank 4 leakage transformer ( $n_{2:3}$ ,  $n_{2:4}$  and  $n_{2:5}$ ), 2 couplers for the rank 3 leakage transformer ( $n_{3:4}$  and  $n_{3:5}$ ) and 1 coupler for the rank 2 leakage transformer ( $n_{4:5}$ ).

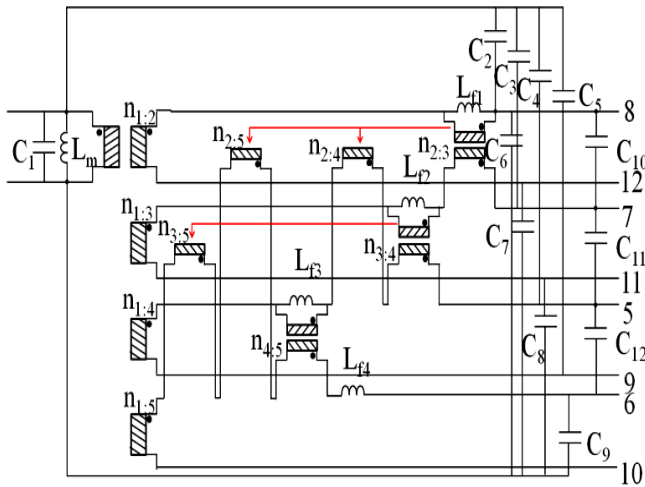


Fig 20 Equivalent circuit of the transformateur T1-4

The 5 inductances ( $L_m$ ,  $L_{f1}$ ,  $L_{f2}$ ,  $L_{f3}$  and  $L_{f4}$ ) and the parasitic capacitances ( $C_1 \dots C_{12}$ ) are the same as calculated in TABLE III and TABLE IV. The ten other parameters

( $n_{1:2}$ ,  $n_{1:3}$ ,  $n_{1:4}$ ,  $n_{1:5}$ ,  $n_{2:3}$ ,  $n_{2:4}$ ,  $n_{2:5}$ ,  $n_{3:4}$ ,  $n_{3:5}$  and  $n_{4:5}$ ) are calculated from the equations obtained by impedance measurements defined in TABLE V.

TABLE V  
MEASUREMENT CONFIGURATIONS OF INDUCTANCES AND COUPLERS

Measure	Coupler	view of the winding	With
$Z_{m6}$	$L_{f1} + n_{1:2}^2 \cdot L_m = \frac{Z_{m6}}{2\pi f} \Big _{\varphi=\pi/2}$	8 to 12	$i1=i3=i4=i5=0$
$Z_{m7}$	$L_{f2} + n_{2:3}^2 \cdot L_{f1} + n_{1:3}^2 \cdot L_m = \frac{Z_{m7}}{2\pi f} \Big _{\varphi=\pi/2}$	7 to 11	$i1=i2=i4=i5=0$
$Z_{m8}$	$L_{f3} + n_{2:4}^2 \cdot L_{f1} + n_{3:4}^2 \cdot L_{f2} + n_{1:4}^2 \cdot L_m = \frac{Z_{m8}}{2\pi f} \Big _{\varphi=\pi/2}$	5 to 9	$i1=i2=i3=i5=0$
$Z_{m9}$	$L_{f4} + n_{2:5}^2 \cdot L_{f1} + n_{3:5}^2 \cdot L_{f2} + n_{4:5}^2 \cdot L_{f3} + n_{1:5}^2 \cdot L_m = \frac{Z_{m9}}{2\pi f} \Big _{\varphi=\pi/2}$	6 to 10	$i1=i2=i3=i4=0$
$Z_{m10}$	$\frac{L_{f1} \cdot \frac{L_{f2}}{n_{2:3}^2}}{L_{f1} + \frac{L_{f2}}{n_{2:3}^2}} = \frac{Z_{m10}}{2\pi f} \Big _{\varphi=\pi/2}$	8 to 12	$i4=i5=0$ and $v1=v3=0$
$Z_{m11}$	$n_{2:3}^2 \cdot L_{f1} + \frac{L_{f2} \cdot \frac{L_{f3} + n_{2:4}^2 \cdot L_{f1}}{n_{3:4}^2}}{L_{f2} + \frac{L_{f3} + n_{2:4}^2 \cdot L_{f1}}{n_{3:4}^2}} = \frac{Z_{m11}}{2\pi f} \Big _{\varphi=\pi/2}$	7 to 11	$i2=i5=0$ and $v1=v4=0$
$Z_{m12}$	$\frac{n_{3:4}^2 \cdot L_{f2} + n_{2:4}^2 \cdot L_{f1} + \frac{L_{f3} \cdot \frac{L_{f4} + n_{2:5}^2 \cdot L_{f1} + n_{3:5}^2 \cdot L_{f2}}{n_{4:5}^2}}{L_{f3} + \frac{L_{f4} + n_{2:5}^2 \cdot L_{f1} + n_{3:5}^2 \cdot L_{f2}}{n_{4:5}^2}}}{L_{f3} + \frac{L_{f4} + n_{2:5}^2 \cdot L_{f1} + n_{3:5}^2 \cdot L_{f2}}{n_{4:5}^2}} = \frac{Z_{m12}}{2\pi f} \Big _{\varphi=\pi/2}$	5 to 9	$i2=i3=0$ and $v1=v5=0$

$Z_{m13}$	$L_{f4} + n_{3,5}^2 \cdot L_{f2} + n_{4,5}^2 \cdot L_{f3}$ $= \frac{Z_{m13}}{2\pi f} \Big _{\varphi=\pi/2}$	6 to 10	$i3=i4=0$ and $v1=v2=0$
$Z_{m14}$	$\frac{L_{f1} \cdot \frac{L_{f3} + n_{3,4}^2 \cdot L_{f2}}{n_{2,4}^2}}{L_{f1} + \frac{L_{f3} + n_{3,4}^2 \cdot L_{f2}}{n_{2,4}^2}}$ $= \frac{Z_{m14}}{2\pi f} \Big _{\varphi=\pi/2}$	8 to 12	$i3=i5=0$ and $v1=v4=0$
$Z_{m15}$	$\frac{n_{2,3}^2 \cdot L_{f1} + \frac{L_{f4} + n_{2,5}^2 \cdot L_{f1} + n_{4,5}^2 \cdot L_{f3}}{n_{3,5}^2}}{L_{f2} + \frac{L_{f4} + n_{2,5}^2 \cdot L_{f1} + n_{4,5}^2 \cdot L_{f3}}{n_{3,5}^2}}$ $= \frac{Z_{m15}}{2\pi f} \Big _{\varphi=\pi/2}$	7 to 11	$i2=i4=0$ and $v1=v5=0$

The results (Fig 21, Fig 22) show a good agreement between measurements and calculations, of electromagnetic disturbances in CM as in DM; thus validating the HF model with leakage inductances.

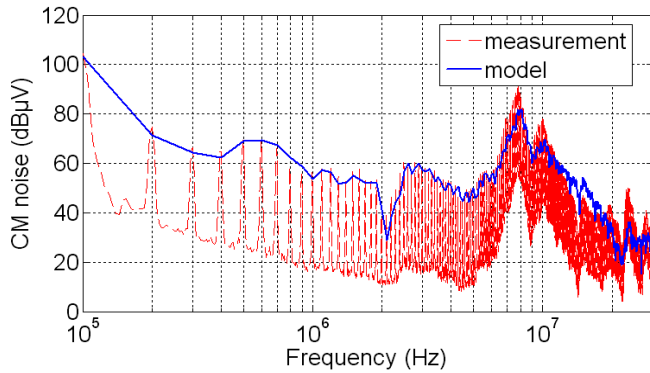


Fig 21 Differential mode noise comparison (model and measurement)

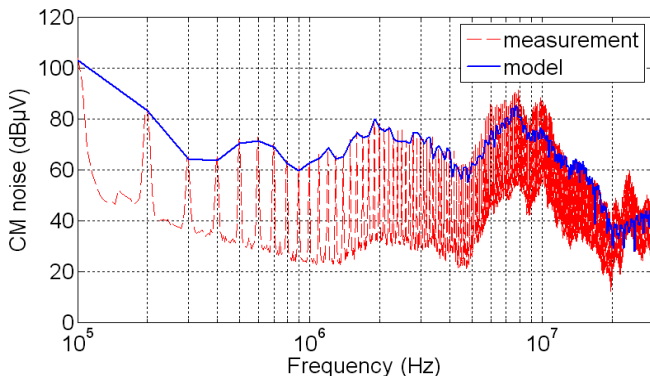


Fig 22 Common mode noise comparison (model and measurement)

## VIII. Conclusion

The main objective of this study is to obtain a HF model to predict the electromagnetic interference generated by switching power supplies with a complex structure.

The studied model replaces: the active components by voltage sources (which are the voltages at transistors and diodes terminals) which are added with parasitic and dynamic impedances and passive components by their HF model.

Two HF models of multi-windings transformer used in switching power supply were presented :

- a model without leakage transformer couplers : used to calculate the differential-mode representing a limit for the common-mode
- and a model with these couplers validated by calculation and measurement comparisons showing the importance of taking into account leakage inductances couplers.

The model accuracy is verified by comparing simulated disturbances and measurements. Good approximation is demonstrated.

This study aims at helping switching power supply designers.

## References

- [1] K.. Mostefaoui-Kasri, Y. Azzouz, A. Louis, B. Mazari, S. alves, P. Eudeline, "Differential-mode conducted EMI generated by SEPIC for radar application," 7th International Workshop on Electromagnetic Compatibility on Integrated Circuits(EMC Compo), France, November 2009.
- [2] P.T.M. Vacasen, "Transformer model of high frequencies," *IEEE Transactions on Power Delivery*, pp. 1761-1768, Vol. 3, July 1982.
- [3] F. De Leon, A. Semlyen, "Complete transformer model for electromagnetic transients", *IEEE Transactions on Power Delivery*, Vol. 9, No. 1, pp. 231-238, January 1994.
- [4] I.A. Maio, P. Savi, I.S. Steivano, F.G. Canavero, "Augmented models of high-frequency transformers for SMPS," 20th International Zurich Symposium on Electromagnetic Compatibility (EMC Zurich), Switzerland, January 2009.
- [5] R. Asensi, J.A. Cobos, P. Alou, R. Prieto, J. Uceda, "Characterization of windings coupling in multi-windings magnetic components," PESC'99, 30th Annual *IEEE Power Elec. Specialists conf*, Vol. 2, No. 1, pp. 753-758, January 1994.
- [6] M. Bartoli, A. Reatti, M. K. Kazimierczuk, "Modeling iron-powder inductors at high frequencies" *MagneTek S.p.A.* 1994 IEEE
- [7] J. Benecke, S. Dickmann "Inductive and capacitive couplings in DC motors with built-in damping chokes". *Colloque CEM Saint-Malo*, France 2006.
- [8] R. Kahoul, Y. Azzouz, P. Marchal and B. Mazari, "Behavioral frequency model of dc motor armature for emc problems". *IEEE Transaction on EMC*, Vol.52, n. 4, November 2010 .
- [9] A. Boglietti and E. Carpaneto, "Induction motor high frequency model," in Proc. Conf. Rec. 1999 *IEEE Int. Conf. Ind. Appl.*, Phoenix, USA, vol. 3, pp. 1551-1558.
- [10] R. kahoul, Y. Azzouz, A. Louis, P. Marchal, B. Mazari, "HF model of DC motor impedance EMC problems in automotive applications" *IEEE EMC 08*, Detroit, USA, August 2008.
- [11] B. Revol, "Modélisation et optimisation des performances CEM d'une association variateur de vitesse - machine asynchrone". Thèse de doctorat de l'Université Joseph Fourier, novembre 2003.

- [12] G. Grandi, K. Kazimierczuk, G. Sancineto, U. Reggiani, "High-Frequency small-signal model of ferrite core inductors," *IEEE Transactions on magnetic*, vol 35, no. 5, september 1999.
- [13] Gabriele Grandi, Marian K. Kazimierczuk, "Model of laminated iron-core inductors for high frequencies," *IEEE Transactions on magnetics*, vol 40, no. 4, july 2004.
- [14] J. L. Guardado, J. A. Flores, V. venegas, J. L. Naredo, "A machine winding model for witching transient studies using network synthesis," *IEEE Transactions on energy conversion*, vol. 20, no. 2, june 2005.

<sup>1</sup>Esigelec/Irseem, Technopole Madrillet, Avenue Isaac Newton 76800 Saint-Étienne-du-Rouvray, France (e-mail: [azzouz@esigelec.fr](mailto:azzouz@esigelec.fr), [mostefaoui\\_kahina@yahoo.fr](mailto:mostefaoui_kahina@yahoo.fr))

<sup>2</sup>University of Brest, EA 4325 LBMS, Rue de Kergoat, CS 93837, 29238 Brest Cedex 03, France (e-mail: [Mohamed.Benbouzid@univ-brest.fr](mailto:Mohamed.Benbouzid@univ-brest.fr)).

<sup>3</sup>Cesi, Centre de Rouen, 76130, Mont Saint Aignan, France (e-mail: [bmazari@cesi.fr](mailto:bmazari@cesi.fr), [alouis@cesi.fr](mailto:alouis@cesi.fr)).

<sup>4</sup>Thales, ZI du Mont Jarret – 76520 Ymare, France (e-mail: [philippe.eudeline@thalesgroup.com](mailto:philippe.eudeline@thalesgroup.com))

## Authors' information



**Kahina MOSTEFAOUI-KASRI** was born in Algiers, on November 13, 1979. She received the Electrotechnical. Eng. dipl. from the University UMMTO, in 2001, the master's Research degree (DEA) in EEA from Paris 11, France, in 2006 and the Ph.D. degree in EMC from the Research Institute for Embedded Systems (IRSEEM), Rouen, France, in 2011.



**Yacine AZZOUC** He received the degree in electrical engineering from the institute of Annaba, Algeria, the M.S. degree in electrical engineering from the National Polytechnic Institute of Toulouse, France, in 1996, and the Ph.D degree in electrical engineering from the university of Aix-Marseille III, France, in 2000. He is currently a professor at the department of Electronic and Systems, Ecole Supérieure d'Ingénieurs-Research Institute for Electronic Embedded systems ESIGELEC/IRSEEM Rouen France



**Mohamed El Hachemi Benbouzid** was born in Batna, Algeria, in 1968. He received the B.Sc. degree in electrical engineering from the University of Batna, Batna, Algeria, in 1990, the M.Sc. and Ph.D. degrees in electrical and computer engineering from the National Polytechnic Institute of Grenoble, Grenoble, France, in 1991 and 1994, respectively, and the Habilitation à Diriger des Recherches degree from the University of Picardie "Jules Verne," Amiens, France, in 2000.

After receiving the Ph.D. degree, he joined the Professional Institute of Amiens, University of Picardie "Jules Verne," where he was an Associate Professor of electrical and computer engineering. Since September 2004, he has been with the Institut Universitaire de Technologie of Brest, University of Brest, Brest, France, where he is a Professor of electrical engineering. His main research interests and experience include analysis, design, and control of electric machines, variable-speed drives for traction, propulsion, and renewable energy applications, and fault diagnosis of electric machines.

Prof. Benbouzid is a Senior Member of the IEEE Power Engineering, Industrial Electronics, Industry Applications, Power Electronics, and Vehicular Technology Societies. He is an Associate Editor of the IEEE TRANSACTIONS ON ENERGY CONVERSION, the IEEE TRANSACTIONS ON INDUSTRIAL ELECTRONICS, the IEEE TRANSACTIONS ON VEHICULAR TECHNOLOGY, and the IEEE/ASME TRANSACTIONS ON MECHATRONICS.

**Anne Louis** was born in Châteauroux, France, in 1973. She received the Ph.D. degree in microwave communications from the Institut de Recherche en Communications Optiques et Microondes, University of Limoges, Limoges, France, in 1998. She joined the 'Ecole Supérieure d'Ingénieurs Généralistes (ESIGELEC), Rouen, France, in 1999, where she is currently a Lecturer. Her current research interests include EMC components such as characterization, modeling, and simulation.

**Belahcene Mazari** was born in Oujda, Morocco, in 1958. He received the Ph.D. degree in electromagnetism from the University of Rouen, Rouen, France, in 1988. Since 1987, he has been a Professor of electromagnetism and electronics with the Graduate Engineering School, 'Ecole Supérieure d'Ingénieurs Généralistes (ESIGELEC), Rouen, France. In 2001, he was involved in the creation of the Research Institute for Electronic Embedded Systems (IRSEEM), Rouen, where he is currently a Manager. His research interests include electromagnetic compatibility in the automotive domain and electromagnetic compatibility of integrated circuits.

**Philippe Eudeline** was born in Honfleur, France, in 1956. He received the Graduate degree from the Engineering School, Ecole Nationale Supérieure de l'Electronique et de ses Applications, Pontoise, France. He was a Microwave Engineer at Thales Air Defence, Ymare, France, developing subassemblies like solid-state transmitters, local oscillators, etc. Since 2000, he has been the Technical Director of the French-Dutch Department, Thales Air Systems Company, Ymare, where he is in charge of the research and development of advanced technologies. He is the author of many technical papers and is the holder of several patents. He is also an Associated Professor of microwave and radar techniques, at ESIGELEC, Rouen, France.